

## Preparation and Characterization of Polyamide 6/Liquid Natural Rubber Blends

G. M. Shashidhara, K. G. Pradeepa

Department of Polymer Science and Technology, Sri Jayachamarajendra College of Engineering, Mysore 570006, India

Correspondence to: G. M. Shashidhara (E-mail: gm.shashi@yahoo.in)

**ABSTRACT:** This study presents a new approach to toughen Polyamide 6 (PA6) by using a low-molecular weight liquid natural rubber (LNR). The LNR is prepared by mastication of pale latex crepe in the presence of 0.5 phr Peptizol 7. The PA6/LNR blend samples are characterized in terms melt flow index, hardness, abrasion resistance, impact strength, flexural strength, tensile strength, and thermal properties. The impact strength of PA6 increases by about 67% upon addition of 10% LNR. The percolation model is applied to study of brittle to ductile transition. The percolation threshold for the brittle to ductile transition of the blend was found to be 14.5 wt % LNR, corresponding to the critical volume fraction of the stress volume,  $V_{sc} = 0.58$ , which is consistent with the calculated value of  $\approx \pi/6$ . The PA6/LNR blends exhibit cavitation and matrix shear yielding, which would be the main contribution to the increases impact strength. © 2013 Wiley Periodicals, Inc. *J. Appl. Polym. Sci.* **2014**, *131*, 39750.

**KEYWORDS:** rubber; blends; polyamides; mechanical properties; differential scanning calorimetry (DSC)

Received 20 October 2012; accepted 10 July 2013

DOI: 10.1002/app.39750

### INTRODUCTION

Polyamides are considered as high strength engineering thermoplastics which find extensive applications in high impact stress parts such as gears, lightly loaded slider pads, hammer heads, pneumatic brake liners, underwater flexible pipes for offshore drilling, industrial pneumatic and hydraulic hose applications, sports items, electrical and electronics devices, and other engineering fields. Although polyamides are ductile at room temperature, they become brittle under severe conditions such as high strain rates and/or low temperatures. This is due to the low crack propagation resistance of polyamides. Polyamide 6 (PA6) is well known for its processibility, high tensile properties, abrasion resistance and chemical resistance. However, poor impact strength of PA6 is the major limitation of its usage in some application in the automotive industry. To overcome this problem, several approaches have been employed to improve the toughness of PA6 which include the addition of tougheners such as different types of rubbers. An appropriate range of rubber particle size, interparticle distance and uniform distribution of the rubber particles plays an important role to achieve the desired extent of toughening. Use of modified rubbers such as styrene ethylene butylene styrene-*g*-maleic anhydride (SEBS-*g*-MAH), polyolefin elastomer-*g*-maleic anhydride (POE-*g*-MAH) in the preparation of binary polyamide/rubber blends has been widely studied to further endow it with advanced and balanced properties.<sup>1,2</sup> PA6/acrylonitrile butadiene styrene (ABS) blends

compatibilized using imidized acrylic polymer,<sup>3</sup> styrene/maleic anhydride copolymer,<sup>4</sup> styrene/acrylonitrile/maleic anhydride terpolymer,<sup>5</sup> maleated poly (methyl methacrylate)<sup>6</sup> have shown improved impact properties. Ethylene propylene diene monomer (EPDM), ethylene propylene rubber (EPM) and polyethylene functionalized with maleic anhydride can be used as an impact modifier for PA6.<sup>7–9</sup> The effect of the maleic anhydride coupling agent on impact behavior of nylon-rubber blends and the brittle-tough transition has been investigated by these authors.

Interest in developing new applications of natural rubber (NR) is intense in natural rubber producing countries. Several reports on the use of NR as an impact modifier can be seen in the literature. Graft copolymer NR-*g*-PA6 prepared in situ by the addition of maleic anhydride to NR at room temperature, prior to blending with PA6 has been reported to be very effective in reducing particle size dramatically.<sup>10</sup> Liquid natural rubber (LNR) has been used as an impact modifier for PVC,<sup>11</sup> PE,<sup>12–17</sup> and epoxy resin.<sup>18</sup> The elastomeric nature of rubber acts as energy dissipating center to cause the ductile fracture for the rubber modified epoxy.<sup>19</sup> The addition of LNR has significantly improved the tensile properties, hardness and degree of cross linking of the blends. Impact modification of PA6 using LNR was reported by Axtell et al.<sup>20</sup> They observed that the dispersion of NR in PA6 was dependent on the viscosity ratio of blends. Shamsuri et al.<sup>21</sup> have prepared PA6/LNR blends via emulsion

technique and confirmed the compatibility of blend based on a single  $T_g$  of the blend. Thus LNR has a potential to be a good compatibilizer in thermoplastic natural rubber (TPNR) blends.

LNR can be prepared by mastication of block rubber. Mastication is a thermo mechanical process wherein long chain elastomer molecules are split to form shorter chains with terminal free radicals. If mastication is carried out in a nitrogen or any other inert gas atmosphere, these short chains recombine into long-chain molecules, whereas if stabilized with radical acceptor or peptizer such as thiophenols or aromatic disulfides, the short ones remain. Because of the high effectiveness of peptizing agents, their dosages are kept very low (0.05–0.15 phr). The peptizers decrease the viscosity of rubbers, promote rapid and good dispersion of fillers and chemicals and increase compound plasticity. Low molecular weight natural rubber (20,000 g/mol) obtained by the above process is commonly known as LNR. The LNR can flow at room temperature and hence mixing process becomes easy.<sup>22</sup> Different strategies are reported in literature to prepare LNR having wide range of molecular weight. Among these, the most common techniques are mastication and reaction with phenyl hydrazine,<sup>20</sup> depolymerization of natural rubber latex using nitrobenzene,<sup>23</sup> thermal degradation of natural rubber latex<sup>24</sup> and depolymerization of NR by the combined action of mechanical and thermal energies aided by a peptizer activated pentachlorothiophenol.<sup>25</sup> Alternatively, LNR can be prepared by irradiating NR solution in toluene with visible light for 10 days.<sup>21</sup>

This study was taken up with an aim to optimize the conditions for preparing LNR of desired molecular weight by masticating pale latex crepe (PLC) in the presence of a commercially available peptizer, Peptizol 7. Blends of PA6 and LNR of different composition (95/05, 90/10, 85/15, and 80/20, all wt %) were prepared via melt route. Another aim of this investigation was to examine the extent of toughening of PA6 by LNR. The PA6/LNR blends were characterized in terms of flow properties, thermal properties, mechanical properties and morphology. The percolation model is applied to study of brittle to ductile transition of PA6/LNR blends.

## EXPERIMENTAL

### Materials

PA6 (Gujlon M 28 RC) was supplied by Gujarat State Fertilizer Company, Vadadara, India. The natural rubber in the form of Ribbed Smoked Sheet (RSS) and Pale Latex Crepe (PLC) (molecular weight:  $\sim 9,60,000$  g/mol) were supplied by Kaduthuruthi Rubber marketing society, Kerala, India. The peptizing agent, Peptizol 7, was purchased from Acme Chem., Panoli, India. Peptizol 7 is a conventional blend of pentachloro thiophenol, organometallic complexes, organic and inorganic dispersing agents. Toluene and formic acid were purchased from SD-fine chem., India, and were used without further purification.

### Preparation of LNR

The LNR was prepared by mastication of known quantities of rubber with or without Peptizol 7, using a lab-scale two roll mill (roll size 15.2 cm  $\times$  33 cm, friction ratio 1 : 14, Sohal Engineering Works Bombay, India) for desired time at room

temperature. The viscosity average molecular weight of LNR was determined using Ostwald Viscometer. For this purpose, a stock solution of masticated rubber was prepared by dissolving a known quantity of rubber in toluene (2.5 g of rubber in 250 mL). Using this stock solution, solutions of different concentrations (0.2, 0.4, 0.6, 0.8, and 1.0 g/dL) were prepared to conduct viscosity measurements. From the intrinsic viscosity  $[\eta]$ , expressed in dL/g, the viscosity average molecular weight,  $M$  was estimated from Mark–Houwink equation

$$[\eta] = KM^\alpha \quad (1)$$

where  $K$  and  $\alpha$  are the constants for the given polymer and solvent. The  $K$  and  $\alpha$  value of  $5 \times 10^{-4}$  and 1.4992 have been used to estimate the viscosity average molecular weight.<sup>26</sup>

### Blending and Injection Molding

PA6 was pre dried in a hot air oven for about 24 h at 100°C. A polymer master batch containing 70 wt % PA6 and 30 wt % LNR, was prepared by mixing required quantities of fresh sample of masticated rubber and predried PA6, in an internal mixer (Polylab Rheomix RC 300P) fitted with roller rotors. The mixing conditions were as follows: temperature 215°C, mixing time 8 min, rotor speed 40 RPM. The PA6/LNR blends of different compositions (100/0, 95/05, 90/10, 85/15, and 80/20) were prepared by melt mixing the required quantities of master batch and PA6 in the internal mixer. The blend obtained from the mixer was cooled and shredded into granules, suitable for injection molding. The test specimens required for hardness, abrasion, impact, flexural, tensile tests were prepared by injection molding using Injection molding machine (Polymechplast-model Gold coin PML-NP-100). The optimized conditions for injection molding were: injection pressure-35 bar, injection time-5 s, temperature in different zones; z1 215°C, z2 220°C, z3 223°C, z4 225°C, and z6 235°C.

### Testing and Characterization

Thin films of pure PA6 and PA6/LNR blends were prepared by solution casting and their Fourier transformed infrared (FTIR) spectra were obtained by scanning from 4000 to 400  $\text{cm}^{-1}$  at a resolution of 32  $\text{cm}^{-1}$  using JASCO 4100 spectrophotometer. The melt flow index (MFI) of PA6 and PA6/LNR blends were determined at 240°C and 2.16 kg load in a standard melt indexer (International Engineering Industries, Bombay, India). The hardness of the samples was determined in accordance with standard ASTM D 2240-05, using hardness tester (Durometer—Shore D, P S I Sales, New Delhi, India). The hardness measurement was taken with a 3-mm thick sample at room temperature. The abrasion resistance test was carried out according to ASTM D 1242-95a, using a plastic abrader (S. C. Dey, Kolkata, India). The weight loss due to abrasion under standard conditions is considered as a measure of abrasion resistance. The impact test at room temperature was carried out for the notched specimens according to standard ASTM D 256-10, using a pendulum impact tester (S. C. Dey). The tensile and flexural tests were conducted using a universal testing machine fitted with a 50 kN load cell (Hounsfield, UK, model H50KM), according to standard ASTM D 638-10 and D790-10,

respectively. For all the tests, at least five specimens were used for each measurement. Thermo gravimetric analysis (TGA) of the polymer samples was conducted using TA Instruments model Q 50 TGA under nitrogen atmosphere. Differential scanning calorimetric (DSC) studies of PA6 and PA6/LNR blends were conducted using TA Instruments model Q150 DSC in nitrogen atmosphere. The samples were subjected to heating cycle (10°C/min) followed by cooling cycle and reheating from -50 to 250°C (for blends) and -50 to 230°C (for neat PA6) at a rate of 10°C/min. Scanning electron microscopy (SEM) of the smooth cut surface of molded blend specimens was conducted using Hitachi SU6600 variable pressure field emission scanning electron microscope. The particle size analysis of dispersed rubber particles in PA6 matrix was carried out manually since the particle boundaries were indistinct. The SEM of tensile fractured samples were obtained using Jeol JSM-6390 scanning electron microscope.

## RESULTS AND DISCUSSION

### Preparation of LNR

Initial studies were conducted to understand the effectiveness of Peptizol 7. It was observed that mastication of RSS in a two roll mill for 5 min in the presence of 0.2 phr Peptizol 7 resulted in nearly 17% reduction in molecular weight as compared to mastication without Peptizol 7 (Table I). Though mastication of natural rubber results in the reduction of molecular weight, the rubber hardens or become stiff spontaneously and the viscosity increases upon storage, due to a process, commonly known as storage hardening. The extent of storage hardening of natural rubber at different storage times was estimated in terms of change in molecular weight. As shown in Table I, the molecular weight of RSS and PLC, determined immediately after mastication, were 32,670 and 41,607, respectively. The molecular weight increased by 95% after 263 h of storage in case of RSS and 78% after 24 h of storage in case of PLC.

For the effective blending of PA6 and NR, the molecular weight of NR should be in the range 15,000–20,000 g/mol.<sup>21</sup> Mastication of PLC with 0.5 phr Peptizol 7 for 27 min yielded LNR of lowest molecular weight 12,275 g/mol (Table I). The resulting LNR was too sticky and difficult to handle. Hence we restricted mastication time to 26 min, which results LNR of molecular weight of 19,355 g/mol. It was observed that, the molecular

weight of masticated PLC increased from 19,355 g/mol to 29,721 g/mol after 72 h of storage, due to storage hardening. The storage hardening is further favored by an increase in temperature and humidity. This reaction is believed to occur due to aldehyde groups present in rubber molecule. These groups react with amino groups of free amino acids and proteins to make cross links. Upon storage, cross linking with individual particles take place, which is known as micro gel formation.<sup>27</sup> The micro gel formation leads to increase the rubber hardness which is directly proportional to the viscosity.

### Fourier Transform Infrared (FTIR) Spectroscopy

IR spectroscopy has proved to be an excellent tool to study the hydrogen bonding behavior in polyamides and polyamide based blends.<sup>28</sup> If the blend is immiscible, the absorption spectrum of the blend will be the sum of those for the components. If the blend is miscible because of the specific interactions, then differences will be noted in the spectrum of the blend relative to the sum of those for the components. The FTIR investigation of a miscible blend will not only reveal the presence of such an interaction, but will provide information on which groups are involved.<sup>28</sup> Typical FTIR spectra of PA6/LNR blend (90/10) and PA6 are shown in Figure 1 and the important peak assignments are presented in Table II. No detailed information can be derived from the order sensitive absorption band in the 500 to 1200 cm<sup>-1</sup> wave number region, while significant changes can be observed for the intensity, wave number position and shape of the C=O and NH absorption bands, as a consequence of change in the hydrogen bonding state. The peaks of free association and bound NH arise at 3301 cm<sup>-1</sup> (Peak 1) and 3063 cm<sup>-1</sup> (Peak 2), respectively, for pure PA6. There is a slight shift of Peak 1 (3301 cm<sup>-1</sup> to 3299.5 cm<sup>-1</sup>) and Peak 2 (3063.5 cm<sup>-1</sup> to 3061.7 cm<sup>-1</sup>) to lower wave numbers in case of PA6/LNR blends. The vibration of IR spectra of the NH stretching band reflects the hydrogen bonding condition of amide groups and the hydrogen bond formation generally shifts to lower frequency due to the N-H stretching modes. This is an important source of information, since hydrogen bonding is a strong intermolecular interaction and should affect the miscibility. The Peak 5 at 1645 cm<sup>-1</sup> is due to the free carbonyl, and the Peak 6 at 1544 cm<sup>-1</sup> arises from the carbonyls that are hydrogen bound.<sup>29</sup> As LNR content increases the two peaks become sharper and shifts slightly toward lower wave number.

**Table I.** Mastication of NR in Presence of Peptizer

Feed	Mastication, time (min)	Observed molecular weight (g/mol) after storing for						
		0 h	24 h	48 h	72 h	91 h	139 h	263 h
RSS	5	88,322	-	-	-	-	-	-
RSS + 0.2 phr Peptizol 7	5	73,486	-	-	-	-	-	-
RSS + 0.2 phr Peptizol 7	15	32,670	-	-	36,437	38,814	42,553	63,841
PLC+ 0.2 phr Peptizol 7	15	41,607	49,652	74,177	-	-	-	-
PLC+ 0.5 phr Peptizol 7	20	27,861	-	-	-	-	-	-
PLC+ 0.5 phr Peptizol 7	22	19,779	-	-	-	-	-	-
PLC+ 0.5 phr Peptizol 7	26	19,355	-	-	29,721	-	-	-
PLC+ 0.5 phr Peptizol 7	27	12,275	-	-	-	-	-	-

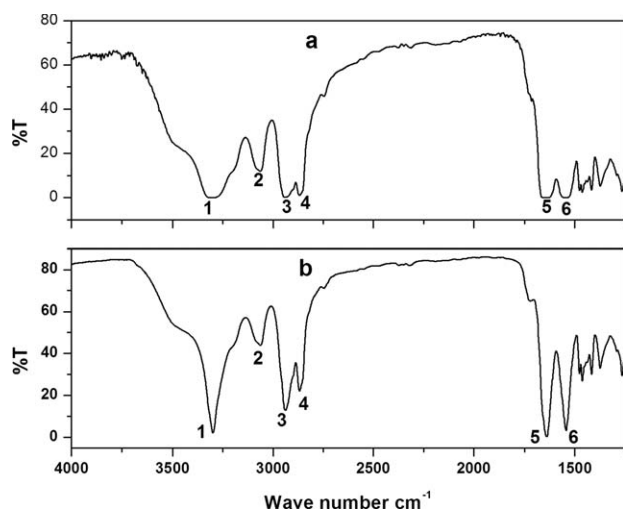


Figure 1. FTIR spectra of (a) PA6 and (b) PA6/LNR blend 90/10.

### Thermal Characterization

The TGA plots showing weight loss as a function of the temperature for PA6, PLC, LNR, and master batch (70/30) are presented in Figure 2. The onset of degradation ( $T_0$ ), the degradation temperature corresponding to 10% weight loss ( $T_{10}$ ) and 50% weight loss ( $T_{50}$ ) are summarized in Table III. The reduction of molecular weight of NR has no influence on thermal stability as we can see the overlapping of thermograms for PLC and LNR. Based on  $T_0$  values, it can be ascertained that the PA6 is thermally stable up to 378°C while 70/30 blend of PA6/LNR is stable up to 332°C. In this study, the melt processing of PA6 and PA6/LNR blends was carried out in the range 215–235°C at which all the polymers under consideration were thermally stable. The DSC thermograms of blends are presented in Figure 3. The peak values melting temperature ( $T_m$ ), enthalpy of melting, and percent crystallinity ( $W_c$ ) and glass transition temperature ( $T_g$ ) are listed in Table IV. The percent crystallinity was calculated using the equation

$$W_c = \frac{\Delta H_m}{w \times \Delta H_{100}} \times 100 \quad (2)$$

where  $\Delta H_m$  is the enthalpy of melting of sample and  $\Delta H_{100}$  is the enthalpy of melting of 100% crystalline PA6 and  $w$  is the weight fraction of PA6 in the Blends. A value of  $\Delta H_{100} = 230$  J/g has been used to calculate the percent crystallinity.<sup>30</sup> Incorporation of amorphous LNR to PA6 lowers the crystallinity. The

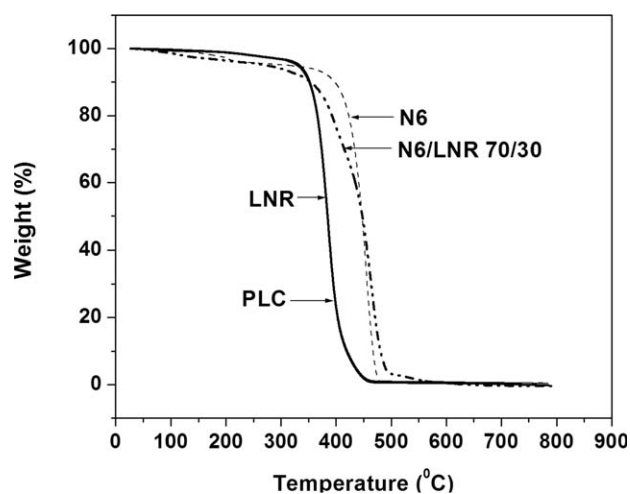


Figure 2. TGA curves.

decrease of crystallinity in blends is attributed to the crystallization of PA6 phase in confined spaces between rubber particles. The melting temperature of blends remains same at around 221°C irrespective of LNR content. In case of blends, a secondary melting peak was observed at around 216°C. The two peaks reflect the formation of two distinct crystal types. The occurrence of multiple melting peaks is more likely when the polymer is scanned using DSC over a temperature range well below the annealing temperature, to above the melting temperature. Under these conditions, semi crystalline polymers can reorganize during DSC scan by a mechanism of partial melting. This is followed by re-crystallization and then ultimately final melting.<sup>31</sup> The glass transition temperature of 95/05 and 80/20 blends were found to be 32.8°C and 31.5°C, respectively. The  $T_g$  of blends decreases slightly with an increase in LNR content.

### Mixing Characteristics of PA6 and LNR

PA6/LNR blends were prepared in an internal mixer. Haake torque rheometry was used to characterize the melt behavior of these materials. Figure 4 shows the characteristic torque versus time curves of PA6/LNR blends. When the polymer mixture is dumped into the mixing chamber, the torque increases instantly to a maximum value, due to shear resistance of blend constituents. When the blend constituents starts melting, the viscosity drops resulting in a reduction in torque. The maximum torque for 95/05, 90/10, 85/15, and 80/20 blends are 31.3, 27.3, 26.4, and 48.7 mm, respectively, indicating a decrease in torque

Table II. IR Frequencies of Pure PA6(100/0) and PA6/LNR Blends

Characteristic groups	Peak number	Peak position (cm <sup>-1</sup> )				
		100/0	95/05	90/10	85/15	80/20
N—H	1	3301	3299	3299.5	3299.5	3299.5
N—H (Bound)	2	3063.5	3062.6	3061.7	3061.7	3061.7
C—H (asymmetric)	3	2941.4	2937.6	2937.6	2938.3	2936.9
C—H (symmetric)	4	2868.2	2867.9	2867.9	2867.5	2866.9
C=O	5	1645	1642	1638.8	1637.6	1637.6
H-bond with carbonyl	6	1544	1543	1542.7	1542.5	1542.5

**Table III.** TGA Data for PA6, PLC, LNR, and PA6/LNR 70/30 Blend

Polymer	$T_0$ (°C)	$T_{10}$ (°C)	$T_{50}$ (°C)
PA6	378	398	448
PLC	330	350	384
LNR	330	350	384
PA6/LNR (70/30)	332	350	448

values with an increase in LNR contents increase up to 15%. The 80/20 blend exhibits relatively higher torque. According to Ibrahim et al, the increase in torque is attributed to the effect of compatibilization.<sup>17</sup> The area under the torque vs. time curve represents the mechanical energy consumed during blending. The energy consumed is highest for 80/20 blend (11 kJ) and is lowest for 95/05 blend (8.7 kJ). From Figure 4, it can be ascertained that the mixing torque remains constant after 3 min indicating proper mixing or homogeneity of the blend. Continuous mixing for 8 min ensures intimate mixing of the blend components.

#### MFI, Hardness, and Abrasion Resistance

Adding rubber particles to a neat polymer melt changes its rheology, influencing both the way the melt processes and the properties of the ultimate product. The key factors are particle size, shape, concentration, and the extent of any interactions among the particles. One of the significant drawbacks of rubber fillers in commercial systems is the tremendous increase in the process viscosity of the matrix.<sup>32</sup> As shown in Table V, MFI of PA6/LNR blends decreases with an increase in LNR content. This is due to the tackiness of rubber which contributes to the development of increased blend viscosity thereby reducing the MFI. The hardness of PA6/LNR blends decreases with an increase in LNR content (Table V). The reduced hardness is attributed to the inclusion of soft rubber phase into the stiff PA6 matrix. In general, as the degree of crystallinity decreases with temperature close to melting point, stiffness, hardness and

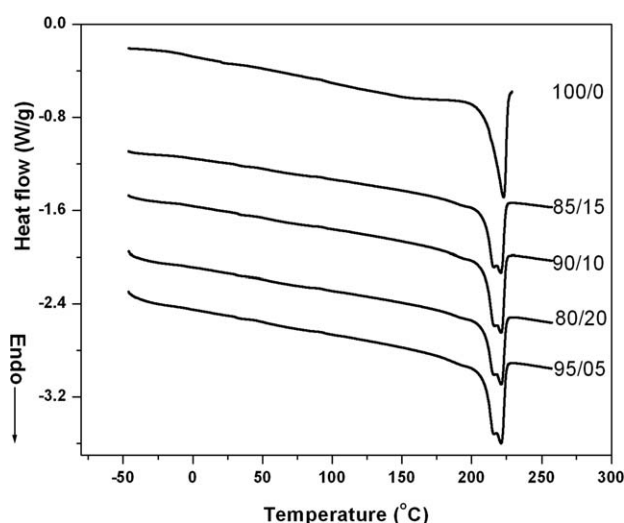
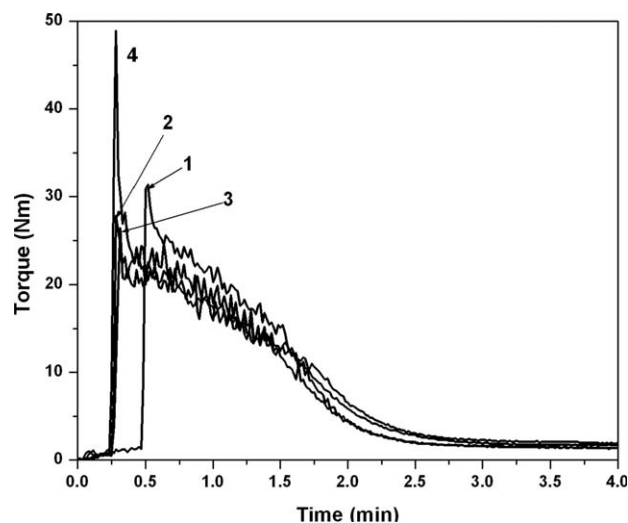
**Table IV.** Melting Temperature, Enthalpy of Melting, Percent Crystallinity, and  $T_g$  of PA6/LNR Blends

Blend designation	$T_m$ (°C)	$\Delta H_m$ (J/g)	$W_c$ (%)	$T_g$ (°C)
95/05	216, 221	48.63	22.25	32.8
90/10	216, 221	42.38	20.47	32.8
85/15	216, 221	39.86	20.38	31.6
80/20	216, 221	38.38	20.85	31.5

yield strength decrease. These factors often set limits on the temperature at which a polymer is useful for mechanical purposes. The abrasion resistance of PA6/LNR blends was measured in terms of volume loss. The addition of LNR up to 20% did not show any significant change in volume loss due to abrasion.

#### Mechanical Properties

For rubber toughened polymers, the shape, content, size and size distribution of the dispersed-phase particles have major effects on mechanical properties of polymer-elastomer blends.<sup>33–35</sup> The Izod impact strength of notched specimens of PA6 and PA6/LNR blends was determined at room temperature and the results are presented in Table V. The impact strength of neat PA6 is 18.46 J/m and that of 95/05, 90/10, and 85/15 blends are 19.82, 30.78, and 30.96 J/m, respectively. Thus, it is apparent that, 5 wt % of LNR in the blend results slight increase (~7%) in impact strength and the blend is still brittle. However, when the dispersed phase, LNR content is increased from 5 to 10%, a sharp brittle ductile transition occurs and the impact strength increase by nearly 67%. After the transition, further increase in the amount of LNR from 10 to 15% does not result in much change in the impact strength. Thus, the impact strength tends to increase with increasing rubber content up to 15%. The presence of soft and flexible particles allows the absorption of energy.<sup>36</sup> The rubber in the blend can cause sufficient stress transfer and thereby preventing the blend from catastrophic failure. The increase in rubber content increases

**Figure 3.** DSC thermograms.**Figure 4.** Characteristic torque versus time curves of PA6/LNR blends. (1) 95/05, (2) 90/10, (3) 85/15, and (4) 80/20.

**Table V.** Mechanical Properties of Pure PA6 and PA6/LNR Blends

Blend	Volume loss (cm <sup>3</sup> )	Hardness shore D	MFI	Impact strength (J/m)	Tensile stress at yield (MPa)	Tensile stress at break (MPa)	Tensile modulus (MPa)	Elongation at break (%)	Flexural strength (MPa)	Flexural modulus (MPa)
100/0	0.09	110	34.8	18.46	50.0	60.0	325	84.0	130	3600
95/05	0.09	68	33.2	19.82	48.4	40.5	319	93.6	103.8	1458
90/10	0.088	66	30.0	30.78	41.7	37.9	299	117.0	88.4	1318
85/15	0.088	64	26.0	30.96	37.6	37.8	269	151.7	83.6	1144
80/20	0.088	60	23.2	>80.0	32.6	32.4	254	209.5	74.9	785

elongation at break and decrease the tensile strength and modulus. The tensile modulus decreases by about 8% upon addition of 10% LNR but there is a 67% increase in impact strength. Though the 80/20 blend shows much higher impact strength, there is a substantial decrease in tensile modulus. Hence 90/10 blend of PA6/LNR can be considered as an optimum composition. The flexural modulus is a measure of stiffness. With the increase in rubber content the flexibility increases but the resistance to withstand bending force decreases. The flexural strength and flexural modulus of PA6 and PA6/LNR blend are given in Table V. Incorporation of 10% LNR, reduced the flexural strength and flexural modulus by 32 and 63%, respectively.

**Brittle Ductile Transition in PA6/LNR Blends.** The fracture toughness of rubber toughened polymers may be attributed to a competition between two deformation mechanisms: crazing and shear yielding.<sup>37</sup> The rubber promotes crazing and shears yielding, which absorbs the energy locally. One of the ways of obtaining the greatest overall toughness in a plastic is by combining shear yielding, crazing, and cracking in the proper order to absorb the highest total energy. Figure 5 reveals the relationship between the impact strength and the weight percent of LNR in PA6/LNR blends. As shown in the figure, an obvious brittle-ductile transition (BDT) of PA6/LNR blends occurs in the Izod impact tests with the increase of LNR content. The value of impact strength nearly unchanged at first and then increased remarkably with increasing LNR content. The point where the rubber content was 14.5% by weight, after which the impact strength enhanced about 3-folds, seems a critical point at which the transition from brittle to ductile behavior in PA6/LNR blends occurred. From this figure, the point where the rubber weight fraction was 0.145, is considered as the critical point. As demonstrated in many polymer/elastomer blending systems, the BDT is controlled by critical surface to surface interparticle distance (ID). For the cubic packing of spherical particles with uniform size, the matrix ligament thickness, i.e. interparticle distance, ID, can be obtained from eq. (3).<sup>38–40</sup>

$$ID = D \left[ \left( \frac{\pi}{6V_r} \right)^{\frac{1}{3}} - 1 \right] \quad (3)$$

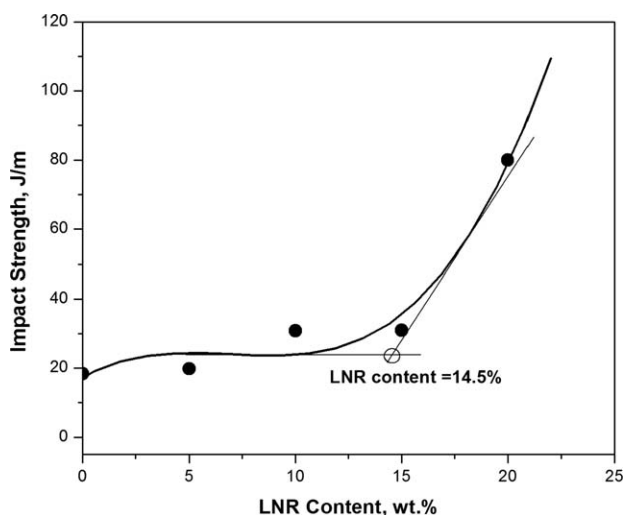
where  $D$  is the rubber particle diameter and  $V_r$  is the rubber volume fraction. The BDT mechanism appears to involve cavitation of rubber particles, which relieves the hydrostatic stresses and thus allows thin matrix ligaments ( $ID < ID_c$ ) to yield locally.<sup>40</sup> The term  $ID_c$  denotes ID at the onset of BDT. When

the thin matrix ligaments are interconnected to form a pervasive network, the yielding process can then propagate and pervade over the entire deformation zone. When this occurs, the blend will exhibit ductile behavior.<sup>40</sup> The concept of the critical ligament thickness that determines whether a blend will be tough or brittle, has been applied to several rubber-toughened polymers, such as nylon and polyvinyl chloride.<sup>39</sup>

SEM was performed on the cut surface of molded blend specimens and the micrographs are shown in Figure 6. The specimen preparation for SEM by cutting, often provides sufficient contrast.<sup>41</sup> The PA6/LNR blends show the uniform distribution of globular rubber particles in the PA6 matrix. The rough texture in micrographs reveals the crystalline character of PA6. The scanning electron micrographs were used to calculate the dispersed-phase particle size. The particles were first traced from the micrograph onto a transparency sheet to obtain the necessary contrast. The number average particle diameter,  $D$ , was calculated using the eq. (4).

$$D = \frac{\sum n_i d_i}{\sum n_i} \quad (4)$$

where  $n_i$  is the number of particles of diameter  $d_i$ . The average diameter of the dispersed rubber particles (in  $\mu\text{m}$ ) in PA6/LNR blends of different compositions were found to be; 2.57 (95/05), 2.16 (90/10), 2.05 (85/15), and 1.77 (80/20). The rubber volume

**Figure 5.** Plot of impact strength versus LNR content in PA6/LNR blends.

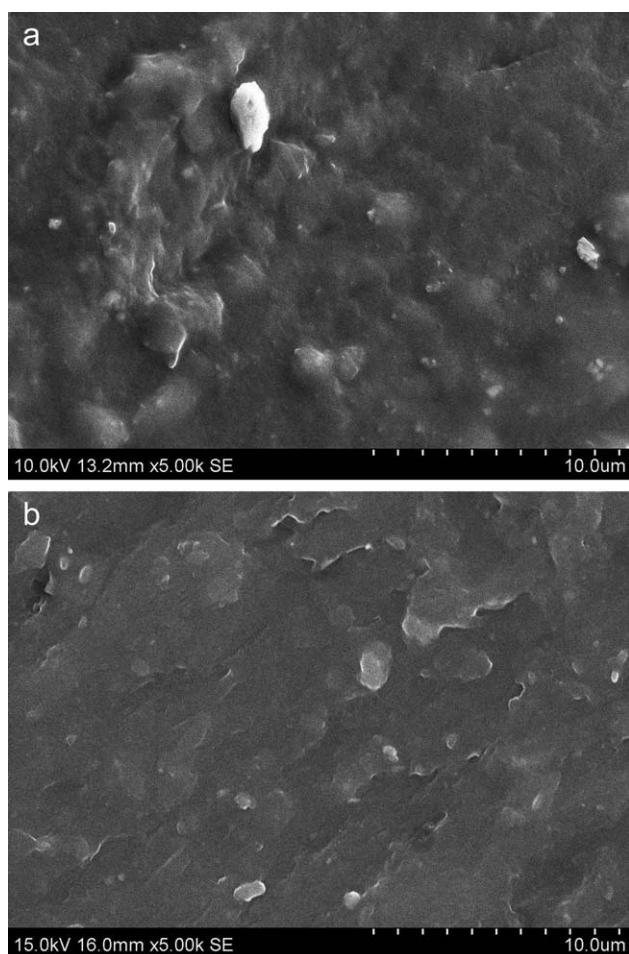


**Figure 6.** SEM micrographs of the cut surface of PA6/LNR blend samples. (a) 95/05 and (b) 90/10.

fraction in PA6/LNR blends,  $V_r$  can be calculated by the eq. (5).<sup>40</sup>

$$V_r = \frac{\rho_m \rho_d}{(\rho_m - \rho_i) w_d + \rho_d} \quad (5)$$

where  $\rho_m$  and  $\rho_d$  are densities of matrix (PA6) and dispersed phase (LNR), respectively,  $w_d$  is the weight fraction of the dispersed phase. The density of PA6 is  $1.14 \text{ g/cm}^3$  and that of NR is  $0.92 \text{ g/cm}^3$ . The critical volume fraction of LNR,  $V_{rc}$ , corresponding to  $w_d = 0.145$  (from Figure 5) is 0.174. The volume fraction of the stress volume ( $V_s$ ) is given by eq. (6).

$$V_s = \left[ \frac{\pi}{6 V_{rc}} \right] V_r \quad (6)$$

When  $V_r = V_{rc}$ , the resulting  $V_s$  is known as the percolation threshold,  $V_{sc}$  ( $= \pi/6 \approx 0.52$ ). From eq. (6), a curve of the relation between impact strength and  $V_s$  can be achieved, as shown in Figure 7. Referring to Figure 7, it can be found that the critical  $V_s$ , i.e. the percolation threshold  $V_{sc}$ , is about 0.58, which is nearly equal to the theoretical value 0.52. In other words, the onset of percolation phenomenon will be observed when LNR content was 14.5 wt %. Thus it is believed that the percolation model is appropriate for the BDT behavior of PA6/LNR blends.

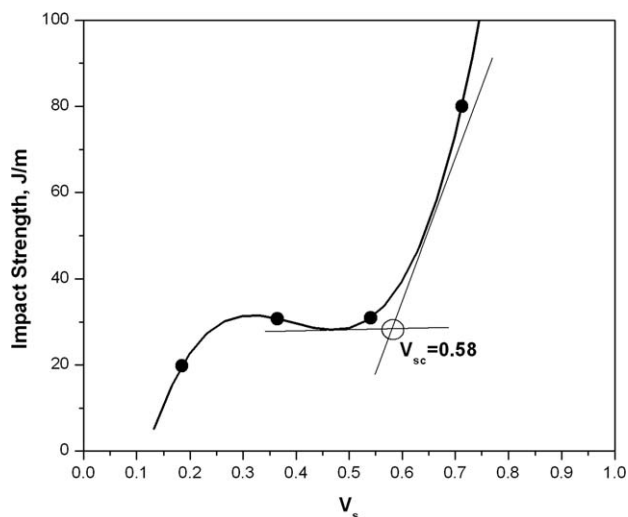


**Figure 7.** Plot of impact strength versus  $V_s$ .

The values of ID (in  $\mu\text{m}$ ) computed by using eq. (3) for PA6/LNR blends of various compositions are as follows; 2.65 (95/05), 1.34 (90/10), 0.86 (85/15), and 0.53 (80/20). The critical interparticle distance,  $ID_c$ , evaluated using eq. (3) with critical values  $D = D_c = 2 \mu\text{m}$ , and  $V_r = V_{rc} = 0.174$  was found to be 0.88. If ID is smaller than  $ID_c$ , then the blend is tough, otherwise the blend is brittle. Hence, the change in ID can induce the BDT of polymers. Generally, the  $ID_c$  not only depends on the properties of the matrix materials, but also depends on the properties of the dispersed phase.<sup>37</sup>

#### Morphology of the Fractured Surface

PA6 and the blends have been examined using SEM. An attempt has been made to correlate the morphology of fracture surface with the tensile properties of the blend systems. The fractographs of PA6 and the blends (95/05, 90/10, 85/15, and 80/20) are given in Figure 8. The tensile fracture surface of neat PA6 [Figure 8(e)] showed that the sample undergoes a brittle mode of failure as the fracture surface is characterized by waviness and closely placed line patterns. The sample undergoes failure without showing a yield point and it has got the highest tensile stress and modulus among all the samples. As the LNR content increases, the brittle fracture changes gradually into a ductile one. With increasing the rubber content to 20%, the fracture front shows an increase of plastic deformation. The fractured surface of the PA6/LNR blends showed very fine phase morphology, so that the boundary between the PA6 and LNR phase cannot be distinctly observed, even when the amount of LNR reaches 20 wt %. The fibrils have been formed by plastic deformation.<sup>42</sup> The orientation of the matrix along the stress axis is also observed at the fracture surface. All these observations indicate that the ductile nature of the blend increases with rubber content. These findings are supported by the respective tensile properties such as tensile stress, modulus and percentage elongation. The tensile stress and modulus decreased and percentage elongation increased with the addition of LNR and thus proved the ductile behavior of blends with the addition of LNR. The dispersed phase in the blend gets more uniformly distributed, and the two phases cannot be distinguished, which is exhibiting

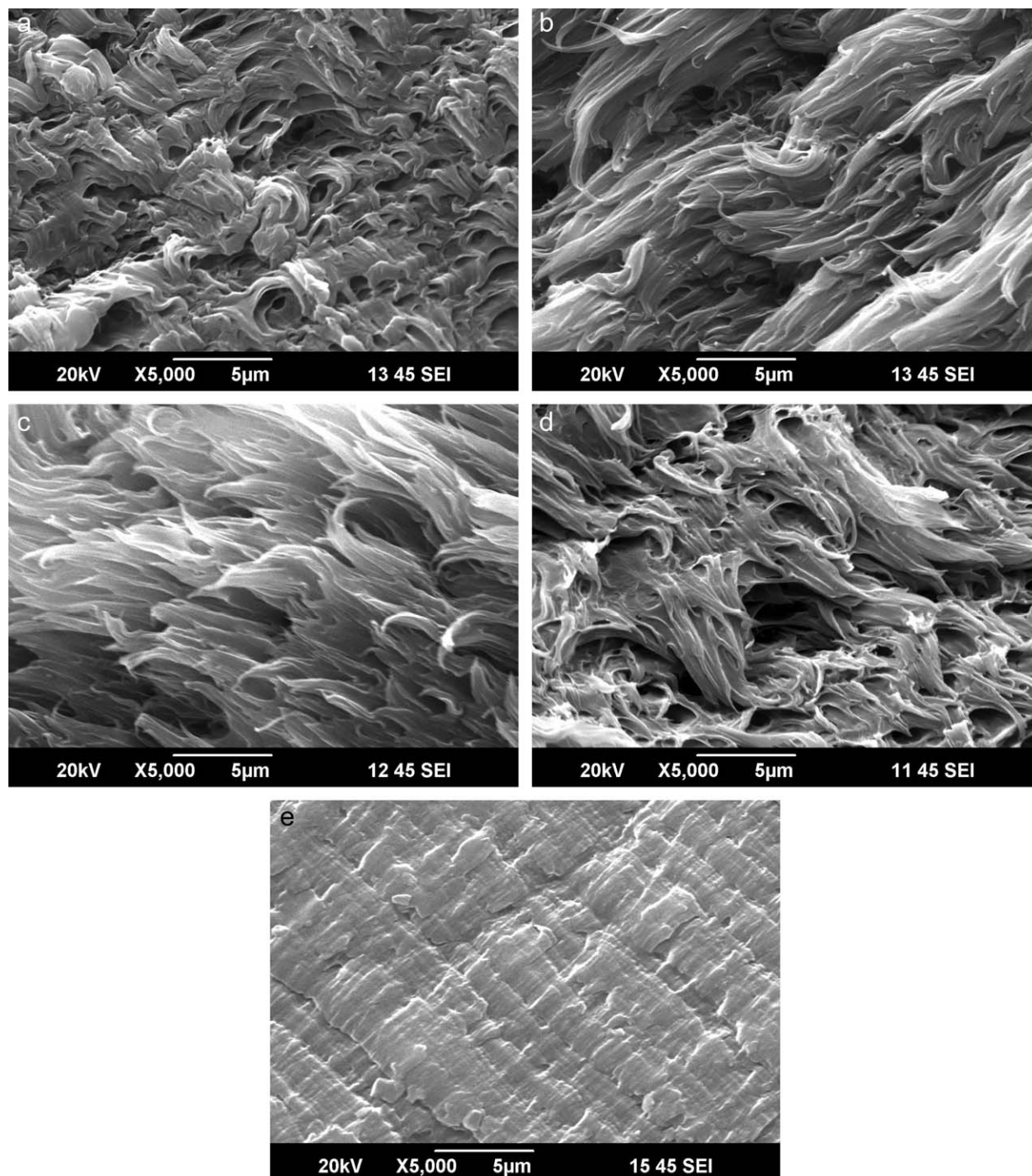


**Figure 8.** SEM micrographs of the fractured surface of PA6/LNR blend samples. (a) 95/05, (b) 90/10, (c) 85/15, (d) 80/20, and (e) 100/0.

the features of the homogeneous blend system. Cavitation and matrix shear yielding appears in Figure 8(a–d), which would be the main contribution to the increases impact strength.

## CONCLUSIONS

The conditions for preparation of LNR were optimized after several trials and strategies. Mastication of PLC with 0.5 phr

Peptizol 7 for 26 min yielded LNR of molecular weight 19,355 g/mol and found to be suitable for melt blending with PA6. Reduction of molecular weight of NR, which occurs during LNR preparation, has no influence on thermal stability as indicated by TGA studies. Based on the thermal stability studies by TGA, the melt processing of PA6/LNR blends can be safely carried out in the range 215–235°C. Intimate mixing of the blend components can be achieved in 8 min in an internal



mixer. The FTIR study shows the vibration at the NH stretching band reflecting the hydrogen bonding condition of amide groups. DSC measurements show reduction in crystallinity of PA6 phase after incorporating LNR to PA6. In the composition range considered, the melting temperature of blends remains same at around 221°C but a secondary melting peak was observed at around 216°C. Addition of LNR to PA6 resulted in a decrease of MFI and hardness of blends while the abrasion resistance increases. The tensile modulus decreases by about 8% upon addition of 10% LNR but there is 67% increase in impact strength. Though the 80/20 blend shows much higher impact strength, there is a substantial decrease in tensile modulus. Incorporation of just 5% LNR reduced the flexural strength and flexural modulus by 20 and 59%, respectively. The curve of Izod impact strength and content of LNR showed a typical brittle to ductile transition phenomenon in PA6/LNR blends. The percolation model has been applied to study the BDT of the PA6/LNR blends. According to the interparticle distance theory and percolation model, the relations of stress volume ( $V_s$ ), and volume fraction ( $V_f$ ) were achieved. It was predicted that the percolation threshold ( $V_{sc}$ ) is about 0.58, which is nearly equal to the theoretical value 0.52. The 14.5 wt % LNR content was a critical point at which the BDT in PA6/LNR blends was induced. The SEM of fractured surfaces of the blends shows a tough type of fracture as indicated by the formation of the fibrils, due to plastic deformation. The orientation of the matrix along the stress axis is also observed at the fracture surface. All these observations indicate that the ductile nature of the blend increases with rubber content. Based on the experimental results and percolation model, it is suggested that a 90/10 blend of PA6/LNR possess balanced properties, making it suitable material for molding of engineering products.

#### ACKNOWLEDGMENTS

The authors thank the Centre Manager, SEM Centre, National Institute of Technology, Calicut, Kerala 673601 and Director, Sophisticated Analytical Instruments Facility, STIC, CUSAT, Cochin 682022, Kerala for using their SEM facility. One of the authors (K.G. Pradeepa) wishes to thank Polymer Processing Academy, India, for Merit Scholarship awarded to this research work.

#### REFERENCES

1. Wu, C. J.; Kuo, J. F.; Chen, C. Y. *Polym. Eng. Sci.* **1993**, *33*, 1329.
2. Wahit, M. U.; Hassan, A.; Mohd Ishak, Z. A.; Czigány, T. *eXPRESS Polym. Lett.* **2009**, *3*, 309.
3. Kudva, R. A.; Keskkula, H.; Paul, D. R. *Polymer* **2000**, *41*, 225.
4. Majumdar, B.; Keskkula, H.; Paul, D. *Polymer* **1994**, *35*, 3164.
5. Jafari, S. H.; Potschke, P.; Stephan, M.; Warth, H.; Alberts, H. *Polymer* **2002**, *43*, 6985.
6. Araujo, E. M.; Hage, E.; Carvalho, A. J. F. *J. Appl. Polym. Sci.* **2003**, *90*, 2643.
7. Dijkstra, K.; Ten Bolscher, G. H. *J. Mater. Sci.* **1994**, *29*, 4286.
8. Guilherme, M. O. B.; Roeder, J.; Soldi, V.; Pires, A. T. N.; Agnelli, J. A. M. *Polímeros [online]* **2003**, *13*, 95.
9. Komalan, C.; George, K. E.; Kumar, P. A. S.; Varughese, K. T.; Thomas, S. *eXPRESS Polym. Lett.* **2007**, *1*, 641.
10. Carone, E., Jr.; Kopcak, U.; Goncalves, M. C.; Nunes, S. P. *Polymer* **2000**, *41*, 5929.
11. Egharevba, O.; Okieimen, F.; Okwu, U.; Malomo, D. *Mater. Sci. Appl.* **2011**, *2*, 196.
12. Dahlan, H. M.; Khairul Zaman, M. D.; Ibrahim, A. *J. Appl. Polym. Sci.* **2000**, *78*, 1776.
13. Sahrim, A.; Ibrahim, A.; Sulaiman, C. S.; Kohjiya, S.; Yoon, J. R. *J. Appl. Polym. Sci.* **1994**, *51*, 1357.
14. Ibrahim, A.; Dahlan, M. *Prog. Polym. Sci.* **1998**, *23*, 665.
15. Qin, C.; Yin, J.; Huang, B. *Polymer* **1990**, *31*, 663.
16. Xanthos, M.; Dagli, S. S. *Polym. Eng. Sci.* **1991**, *31*, 929.
17. Ibrahim, A.; Sahrim, A.; Sulaiman, C. S. *J. Appl. Polym. Sci.* **1995**, *58*, 1125.
18. Kwanming, K.; Klinpituksa, P.; Waehamad, W. *Songklanakarin J. Sci. Technol.* **2009**, *31*, 49.
19. Seng, L. Y.; Ahmad, S. H.; Rasid, R.; Noum, S. Y. E.; Hock, Y. C.; Tarawneh, M. A. *Sains Malaysiana* **2011**, *40*, 679.
20. Axtell, F. H.; Phinyocheep, P.; Monthachitra P. *J. Sci. Soc. Thailand* **1992**, *48*, 195.
21. Shamsuri, A. A.; Daik, R.; Ahmad, I.; Hafizuddin, M.; Jumali, H. *J. Polym. Res.* **2009**, *16*, 381.
22. Hussin, M. N.; John, R. E. *Prog. Polym. Sci.* **1998**, *23*, 143.
23. Okieimen, F. E.; Akinlabi, A. K. *J. Appl. Polym. Sci.* **2002**, *85*, 1070.
24. Siti, Z. I.; Rosiyah, Y.; Aziz, H.; Tahir, M. *Malaysian J. Anal. Sci.* **2007**, *11*, 42.
25. Radhakrishnan Nair, N.; Claramma, N. M.; Mathew, N. M.; Thomas, S.; Someswara Rao, S. *J. Appl. Polym. Sci.* **1995**, *55*, 723.
26. Mark, J. E., Ed. *Polymer Data Handbook*; Oxford University Press: New York, **1998**, p 614.
27. Burfield, D. R. *J. Nat. Rubber Res.* **1986**, *1*, 202.
28. Al-Rawajfeh, A. E.; Al-Salah, H. A.; Al-Rhael, I. *Jordan J. Chem.* **2006**, *1*, 155.
29. Coates, J. In *Encyclopedia of Analytical Chemistry*; Meyers, R. A., Ed.; Wiley: Chichester, **2000**; p 10815.
30. Alexander, J. J.; Anqiu, Z.; Zongquan, W. In *Handbook of Thermal Analysis and Calorimetry: Applications to Polymers and Plastics*; Stephen, Z. D. C., Eds.; Elsevier: Amsterdam, **2002**; *3*, p 441.
31. Scheirs, J. *Compositional and Failure Analysis of Polymers: A Practical Approach*; Wiley: England, **2000**; p 125.
32. George, S.; Ramamurthy, K.; Anand, J. S.; Groeninckx, G.; Varughese, K. T.; Thomas, S. *Polymer* **1999**, *40*, 4325.
33. Stricker, F.; Thomann, Y.; Mulhaupt, R. *J. Appl. Polym. Sci.* **1998**, *68*, 1891.

34. van der Waal, A.; Verheul, A. J.; Gaymans, R. J. *Polymer* **1999**, *40*, 6057.
35. Liang, J. Z.; Li, R. K. *J. Appl. Polym. Sci.* **2000**, *77*, 409.
36. Shashidhara, G. M.; Kameshawari devi, S. H. *Indian J. Eng. Mater. Sci.* **2011**, *18*, 69.
37. Guo, Z.; Fang, Z.; Tong, L. *eXPRESS Polym. Lett.* **2007**, *1*, 37.
38. Wu, S. J. *Appl. Polym. Sci.* **1988**, *35*, 549.
39. Mae, H.; Omiya, M.; Kishimoto, K. In Proceedings of the XIth International Congress and Exposition, June 2–5, **2008** Orlando, FL.
40. Yu, Z.-Z.; Lei, M.; Ou, Y.; Yang, G. *Polymer* **2002**, *43*, 6993.
41. Vesely, D. *Polym. Eng. Sci.* **1996**, *36*, 1586.
42. Biju, P. K.; Radhakrishnan Nair, M. N.; Thomas, G. V.; Gopinathan nair, M. R. *Mater. Sci.-Poland*, **2007**, *25*, 919.